Electronic Supplementary Information

Partially fluorinated poly(arylene-alkane)s containing cobaltocenium for alkaline-stable anion exchange membranes

Run Zhang,[ab] Xiaoyu Zhao,[ab] Wenhao Li,[abc] Huidong Qian*[ab] and Hui Yang*[ab]

[a]Shanghai Advanced Research Institute, Chinese Academy of Sciences, Shanghai 201210, China. *Corresponding author. E-mail: qianhd@sari.ac.cn

[b]University of Chinese Academy of Sciences, Beijing 100049, China

[c]School of Physical Science and Technology, ShanghaiTech University, Shanghai 201210, China

Table of Contents

Experimental section

Materials

Cobaltocene hexafluorophosphate (Cp$_2$CoPF$_6$) was synthesized according to a previous literature report,[1] 1,1,1-trimethylhydrazine iodide (97%), potassium carbonate anhydrous (K$_2$CO$_3$, 98%), potassium tert-butoxide anhydrous (t-BuOK, 98%), p-triphenylene (TP, 99%), biphenyl (BP, 98%), pentafluorobenzaldehyde (PFBA, 98%), trifluoromethane sulphonic acid (TFSA, 98%), 1,1,1-trifluoroacetone (98%), ether (99%), dichloromethane anhydrous (DCM, 99%), tetrahydrofuran anhydrous (THF, 99%), dimethylacetamidemethanol (DMAc, 98%) were purchased from Adamas-beta and used as received.

Synthesis of aminocobaltocene hexafluorophosphate (H$_2$N-Cp$_2$CoPF$_6$)

Prepared Cp$_2$CoPF$_6$ (3.5 g, 10 mmol) and 1,1,1-trimethylhydrazine iodide (2.02 g, 10 mmol) was first added to a 500 mL three-necked flask containing 300 mL THF under N$_2$ atmosphere, followed by anhydrous potassium t-BuOK (1.12 g, 10 mmol), which changed from yellow to purple-black. The solvent and volatiles were spun off on a rotary evaporator, the residue was dissolved in dichloromethane, and the insoluble material was filtered out. The filtered solution was spun dry and dissolved by adding a small amount of acetonitrile and the neutral alumina pretreated with acetonitrile in a short column (column width: 6 cm, column height: 12 cm). First, petroleum ether was used as an eluent to remove the cobaltocene salt and other impurities. Then the pure product (Rf = 0.75) was eluted with acetonitrile as a yellow-orange crystalline substance (yield: 40%).

Synthesis of aliphatic polymers with pentafluorophenyl pendent groups (PFTP)

PFBA (1.71 g, 12 mmol), TP (2.30 g, 10 mmol), TFSA (4 mL), and DCM (8 mL) were added to a 100 mL three-necked flask and stirred for 30 min at 0 °C. The resulting viscous green liquid was slowly poured into methanol. A white fibrous solid was precipitated, washed to neutral, and dried in a vacuum oven at 60 °C for 24 h (yield: 94 %).

Synthesis of PFTP-Cp$_2$Co$_{0.8}$ and preparation of membrane

The prepared PFTP (0.40 g, 1 mmol) was added to a 100 mL three-necked flask containing 10 mL DMAc and heated at 80 °C to dissolve, followed by the addition of $H_2N\text{-}Cp_2CoPF_6$ (0.28 g, 0.8 mmol) and K_2CO_3 (0.11 g, 0.8 mmol). The solution was reacted for 2 h, left to cool, filtered, evacuated, poured onto a glass plate, and dried at 60 °C for 12 h. Other samples were prepared in a similar procedure. The reacted polymer solution (sol) is directly filtered to obtain a transparent and homogeneous red-brown membrane by a typical casting process. Furthermore, the membranes (gel) are first placed in 1 M NH_4Cl solution for 48 h to exchange $PF6^-$ to Cl^-, then in 1 M KOH solution to exchange to OH^- form.

Preparation of the ionomer

Poly[(fluorene alkylene)-co(biphenyl alkylene)] (PFBA) with quaternary ammonium (PFBA-QA) was selected as the ionomer for the preparation of membrane electrode assemblies (MEAs). The synthesis process of the 9,9-bis (6-bromohexyl)-9H-fluorene and PFBA-QA is followed by the previously reported procedure.[2] The IEC of the polymer was adjusted by controlling the ratio of fluorenyl monomer to biphenyl (7:3). The specific synthesis process of PFBA-QA$_{0.7}$ was as follows: BP (0.46 g, 3 mmol), 9,9-bis (6-bromohexyl)-9H-fluorene (3.44 g, 7 mmol), and 1,1,1-trifluoroacetone (1.34 g, 12 mmol) were added in 100 mL three-necked flask in 0°C. Afterward, 8 mL of DCM was added, and 8.4 mL of TFSA was added after the complete dissolution of the substrate. Subsequently, it was stirred for 30 min at room temperature. The obtained gray-green viscous material was poured into methanol and precipitated, followed by drying in a vacuum oven at 60°C for 24 h (yield: 96%). The prepared PFBA (1.95 g, 5 mmol) was dissolved in 30 mL DMAc, followed by the addition of 30% trimethylamine (1.30 g, 20 mmol) dropwise. The solution was stirred for 24 h, poured into the ether to precipitate the solid, and dried in a vacuum oven for 24 h (yield: 90%) (Fig. S8, ESI†). The 5 wt % ionomer was prepared by dissolving 1 g of PFBA-QA$_{0.7}$ in 19 g of isopropanol.

Characterization

Nuclear magnetic resonance (NMR)

The synthesized $H_2N-Cp_2CoPF_6$ was identified by NMR (Bruker AvanceIII 400MHz) using DMSO-d_6 as the solvents, PFTP using CDCl$_3$ as the solvent, and PFBA-QA$_{0.7}$ using DMSO-d_6 as the solvent.

Fourier transform infrared (FT-IR) spectra

FT-IR analysis of PFTP membrane, PFTP-Cp$_2$Co$_{0.8}$ membrane, and alkali-treated PFTP-Cp$_2$Co$_{0.8}$ membrane was carried out using a Nicolet iS50 FT-IR spectrometer under ambient conditions with a resolution of 5 cm^{-1} and a spectral range of 4000-600 cm^{-1}.

UV–visible spectroscopy (UV-vis)

UV-vis analysis was carried out using a UV-vis 8000s Spectrophotometer under ambient conditions with a wavelength range of 800-200 nm.

X-ray photoelectron spectroscopy (XPS)

Elemental cobalt valence analysis was conducted on the Thermo Scientific K-Alpha XPS.

Gel permeation chromatography (GPC)

The molecular weight of polymer was acquired by gel permeation chromatography (GPC, Agilent PL-GPC50) using CHCl$_3$ as an eluent with a flow rate of 1 mL min^{-1}.

Thermogravimetic analysis (TGA) and derivative thermogravimetric (DTG)

A thermal stability test of the PFTP-Cp$_2$Co$_x$ membrane was conducted with a Shimadzu TGA-50H analyzer at a heating rate of 10 °C min^{-1} from 50 to 800 °C under the N$_2$ atmosphere.

Electro-mechanical universal testing machines (EUTM)

The mechanical property, including tensile strength (TS) and elongation at break (Eb) of a fully hydrated membrane, was recorded on an AGS-X-50N at a stretch rate of 1 mm min^{-1}.

Ion exchange capacity (IEC)

The theoretical ion exchange equivalent (IEC[a]) is the molarity of the Cp$_2$Co$_x$ membranes divided by the weight of the membrane. In contrast, the titrated ion exchange equivalent (IEC[b]) of the PFTP-Cp$_2$Co$_x$ membranes were determined by

counter-ion titration. The PFTP-Cp$_2$Co$_x$ membranes were first immersed in 1 M NH$_4$Cl for 48 h to completely exchange to the Cl$^-$ form, followed by immersed in 1 M NaOH solution for 48 h to exchange to the OH$^-$ form completely. Then the membranes were washed with ultrapure water, soaked to remove residual OH$^-$ on the surface, and dried in a vacuum oven for 24 h to get the dry weight (m_{dry}). The samples were soaked in a hydrochloric acid solution (0.01 M) for 48 h, and the remaining hydrochloric acid was titrated with 0.01 M NaOH using phenolphthalein as the indicator. The IEC is calculated by the equation:

$$\text{IEC (mmol/g)} = \frac{0.01 \times (v_{\text{HCl}} - v_{\text{NaOH}})}{m_{\text{dry}}}$$

Water Uptake (WU) and Swelling Ratio (SR)

AEMs (1 cm × 5 cm, in OH$^-$ form) were dried at 80°C for 24 h, and weights (W_d) and lengths (W_d) were recorded, followed by immersion in deionized water at different temperatures for 24 h. After the surface was wiped by filter paper, the weights (W_w) and lengths (L_w) were immediately determined. The water uptake of the AEM is calculated as follows:

$$\text{WU (\%)} = \frac{(W_w - W_d)}{W_d} \times 100\%$$

Where W_w and W_d are the weights of AEMs in the wet and dry states, respectively. The swelling ratio of the AEMs is calculated by the formula:

$$\text{SR (\%)} = \frac{L_w - L_d}{L_d} \times 100\%$$

Where L_w and L_d are the lengths of AEMs in wet and dry states, respectively.

Hydroxide conductivity

The conductivity of the membrane (1 cm × 5 cm, in OH$^-$ form) was measured by a four-probe resistance test (Solatron 1260+1287, UK) in the range 1-10^5 Hz with disturbance potential of 10 mV at different temperature. The conductivity is calculated according to the following equation：

$$\sigma \ (mS \ cm^{-1}) = \frac{d}{R \times A}$$

Where d is the distance of two electrodes (cm), R is the ohmic resistance of the as-prepared membrane (Ω), and A is the effective area of AEM for ion transport (cm^2).

Alkaline stability

The AEM (1 cm × 5 cm) was immersed in a 1 M KOH solution at 80 °C, and the conductivity of the membrane was measured periodically to determine the alkaline stability by the change in conductivity. The FT-IR spectra of the AEM before and after immersion were also tested to observe the degradation of the membrane.

Transmission electron microscopy (TEM)

Sample preparation for TEM testing: The 2 wt % membrane solution was dropped onto the copper mesh and dried in an oven at 60°C for 1 h. The copper mesh was dried without staining treatment for testing. Electron micrographs were taken with a JEM-2100 transmission electron microscope operating at 200 kV.

Electrostatic potential (ESP) calculations

The theoretical calculations were performed via the Gaussian 16 suite of programs.[3] The studied molecules' structures (M1, M2, M3) were fully optimized at the B3LYP-D3BJ/def2-SVP level of theory. The solvent (H_2O) effect was included in the calculations based on the Polarizable Continuum Model (PCM) using the integral equation formalism variant (IEFPCM). The vibrational frequencies of the optimized structures were carried out at the same level. The structures were characterized as a local energy minimum on the potential energy surface by verifying that all the vibrational frequencies were absolute. The Visual Molecular Dynamics (VMD) program[4] was used to plot the color-filled iso-surface graphs to visualize the molecular electrostatic potential (MESP) calculated at the B3LYP-D3BJ/def2-TZVP level. The ESP surface maxima of the molecules were depicted as yellow points, which were calculated based on the optimized structure.

Fuel cell performance

The 5 wt % ionomer solution was prepared by dissolving the PFBA-QA$_{0.7}$ polymer in isopropanol. Catalysts inks were prepared by sonicating the dispersion catalyst (cathode: 5 mg 60% Pt/C catalyst, Johnson Matthey Co.; anode: 5 mg 70% Pt-Ru/C catalyst, Johnson Matthey Co.) and 25 mg of 5 wt % ionomer in 150 mg of

isopropanol/water (w/w = 4/1) solution. The MEAs were prepared by the catalyst-coated substrate (CCS) method by sonicating a mixture of catalyst inks and spraying them onto the gas diffusion electrodes (GDEs, Sigracet 22 BB, SGL Carbon) on a vacuum-heated platform, followed by hot-pressing the AEM and two sides of GDEs at 110 ºC and 3 MPa for 3 min. The cathode and anode catalyst loadings were calculated by weighing the net weight of the GDEs before and after spraying, respectively. Anion exchange membrane fuel cell (AEMFC) performance were carried out at 80°C and 100% relative humidity without backpressure. Hydrogen (400 sccm) and air (or O_2) (400 sccm) were fed as the fuel and oxidizer, respectively.

The membrane electrode catalyst loading is calculated according to the following equations:

$$L_c \text{ (mg cm}^{-2}) = \frac{0.6 \times 0.8 \times m_c}{2.5 \times 2.5}$$

$$L_a \text{ (mg cm}^{-2}) = \frac{0.7 \times 0.8 \times m_a}{2.5 \times 2.5}$$

Where m_c and m_a are the net weight before and after cathode and anode spraying, respectively; L_c and L_a are the cathode and anode catalyst loadings, respectively.
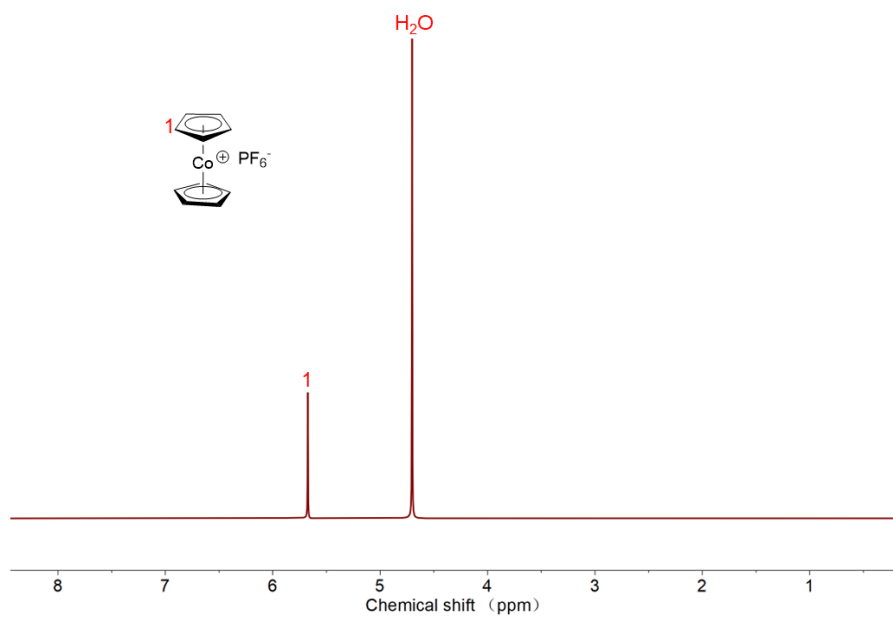
Fig. S1 ^{1}H NMR spectra of Cp_2CoPF_6.
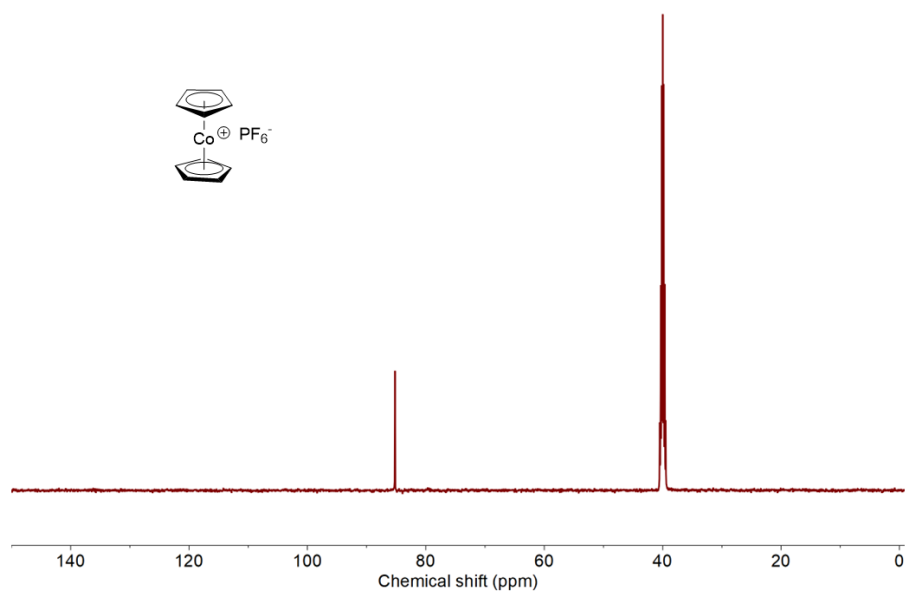
Fig. S2 ^{13}C NMR spectra of Cp_2CoPF_6.
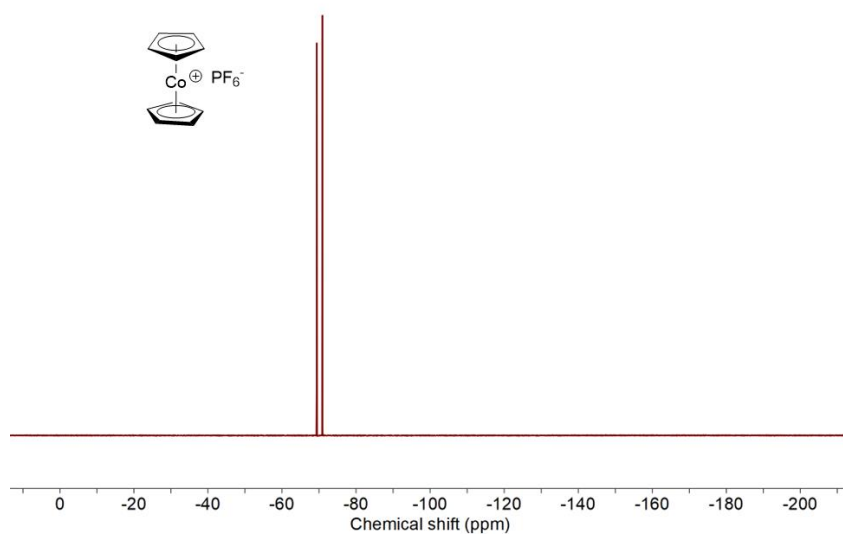
Fig. S3 ^{19}F NMR spectra of Cp_2CoPF_6.
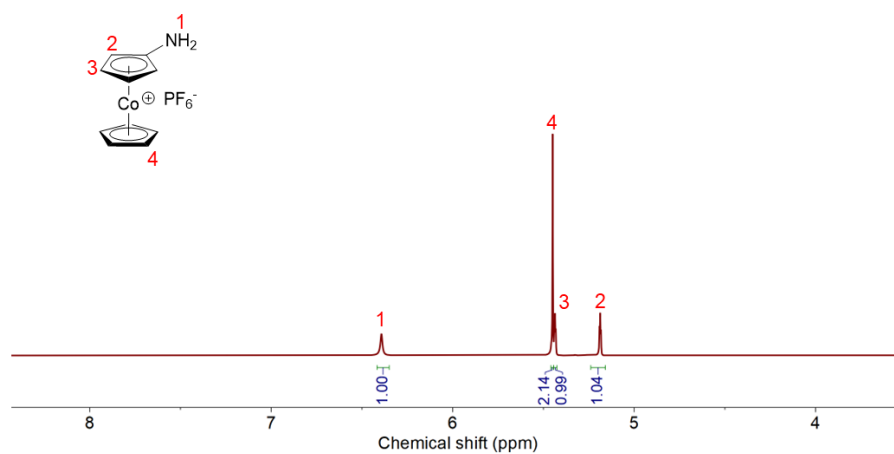
Fig. S4 ^{1}H NMR spectra of H_2N-Cp_2CoPF_6.
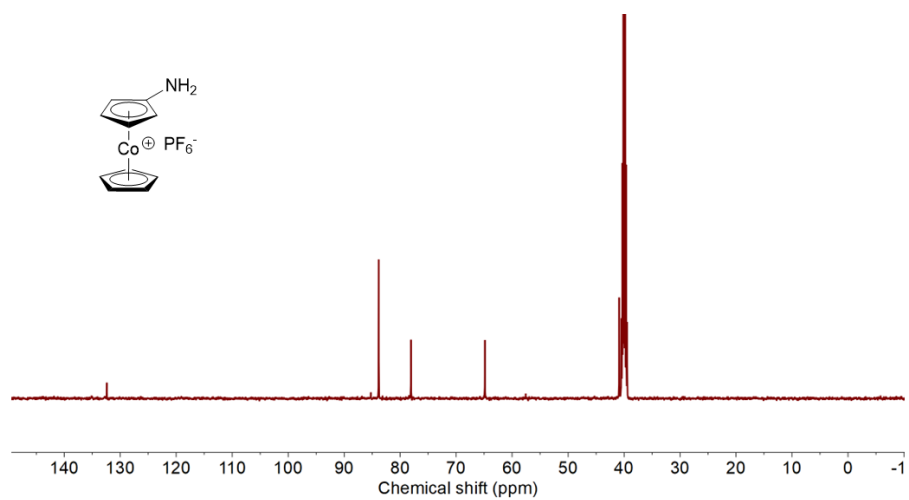
Fig. S5 ^{13}C NMR spectra of H_2N-Cp_2CoPF_6.
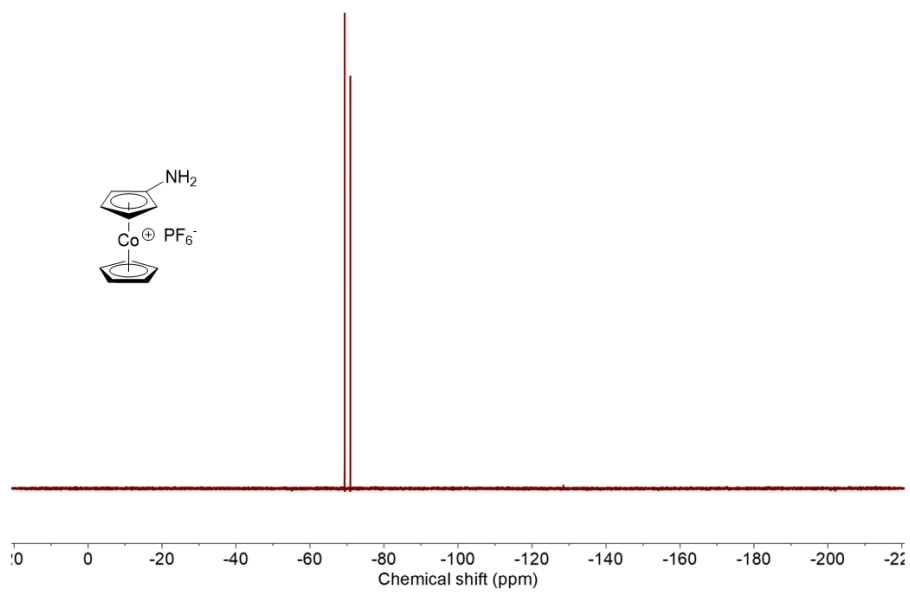
Fig. S6 ^{19}F NMR spectra of H_2N-Cp_2CoPF_6.
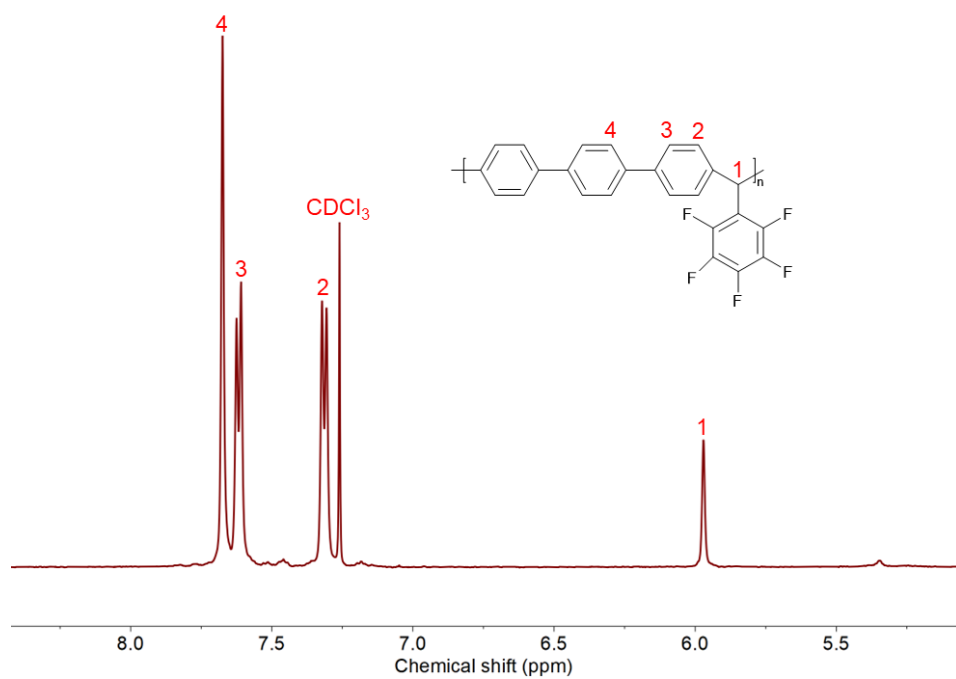
Fig. S7 ^{1}H NMR spectra of PFTP membrane.
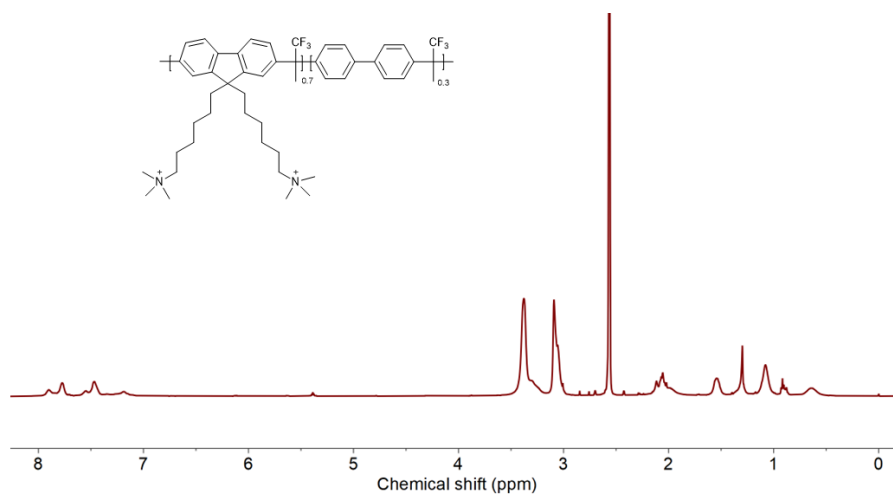
Fig. S8 ^{1}H NMR spectra of PFBA-QA$_{0.7}$.
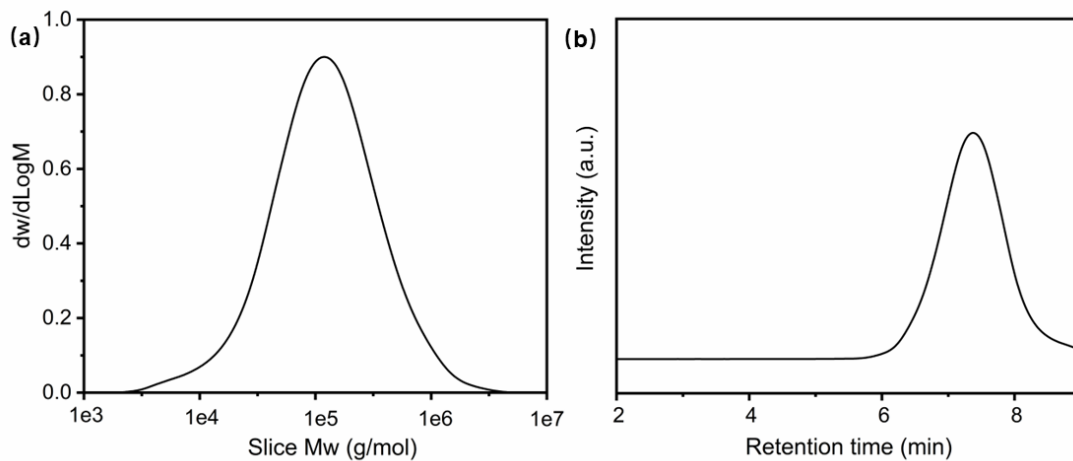
Fig. S9 GPC curves of PFTP. The number-average molecular weight M_n = 63 kDa, weight-average molecular weight M_w = 208 kDa, polydispersion index PDI = M_w/M_n = 3.3.
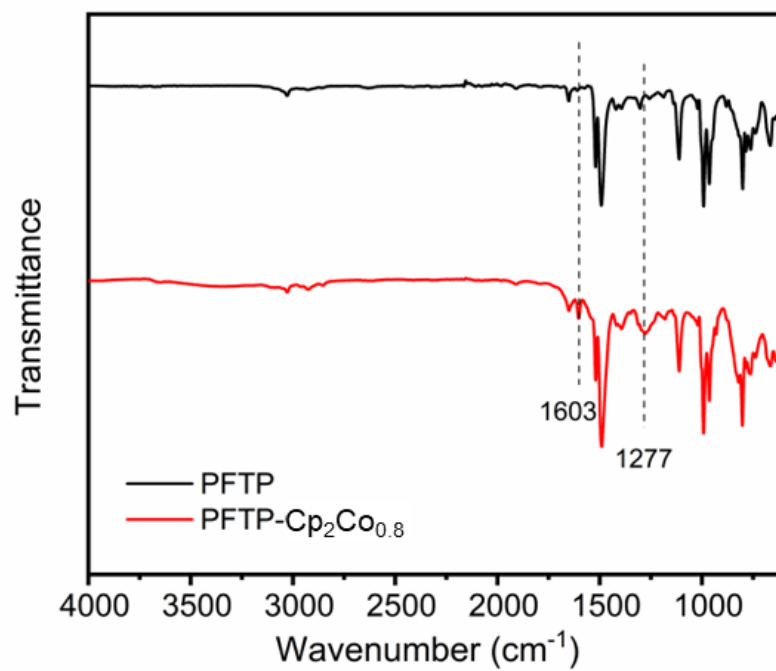
Fig. S10 FT-IR spectra of PFTP membrane and PFTP-Cp$_2$Co$_{0.8}$ membrane.
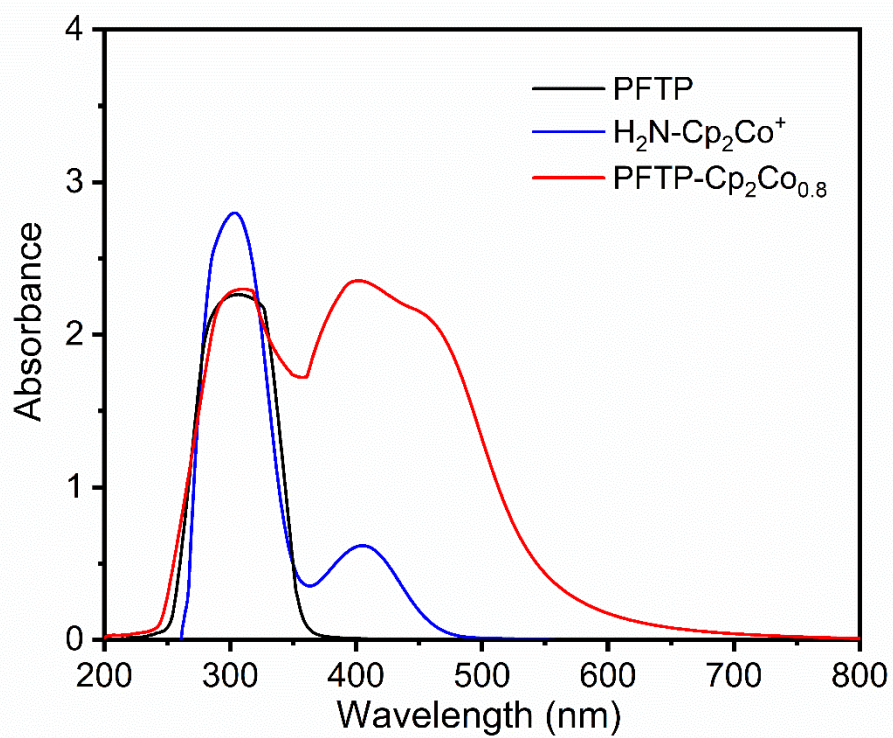
Fig. S11 UV-vis spectra of PFTP membrane, $H_2N-Cp_2Co^+$, and PFTP-$Cp_2Co_{0.8}$ membrane.
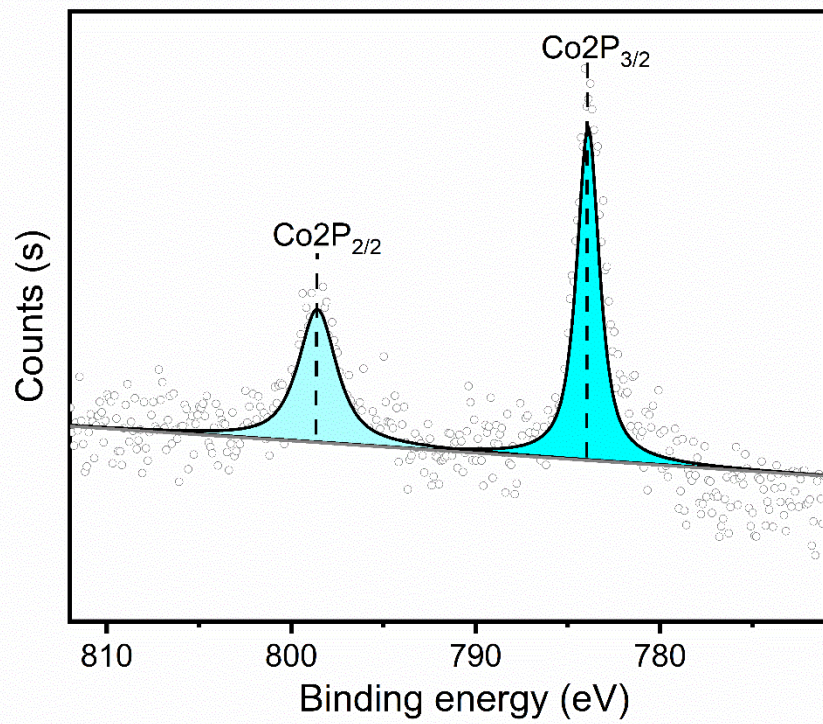
Fig. S12 XPS spectra of Co2P for the PFTP-Cp$_2$Co$_{0.8}$ membrane.
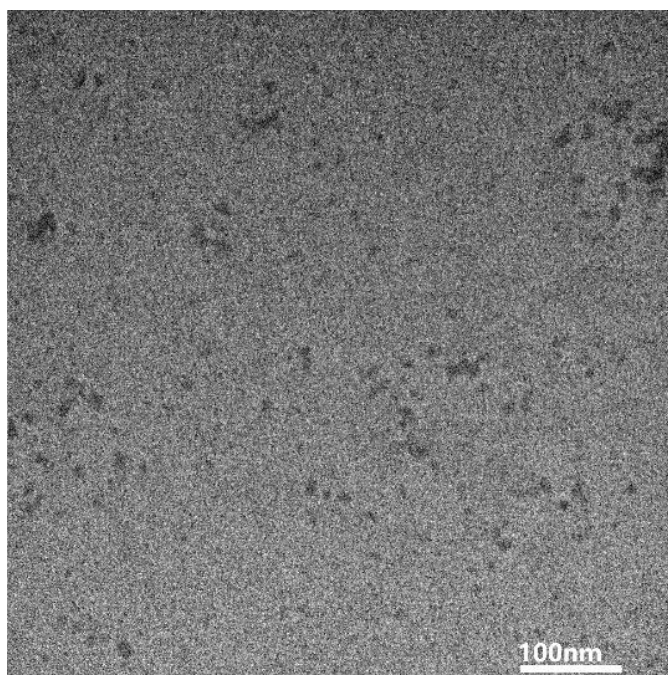
Fig. S13 TEM image of PFTP-Cp$_2$Co$_{0.8}$ membrane.

The dark domains are the hydrophilic segments of cobaltocenium clusters, and the brighter domains are the skeletal hydrophobic segments. The well-developed microphase separation is formed to construct a continuous hydrophilic channel due to the significant distinction of hydrophilic cobaltocenium side chains and the partially fluorinated hydrophobic skeletons. The motion of OH$^-$ in the membrane is promoted by vehicular diffusion in the hydrophilic channel, thus the OH$^-$ conductivity of the membrane is increased.
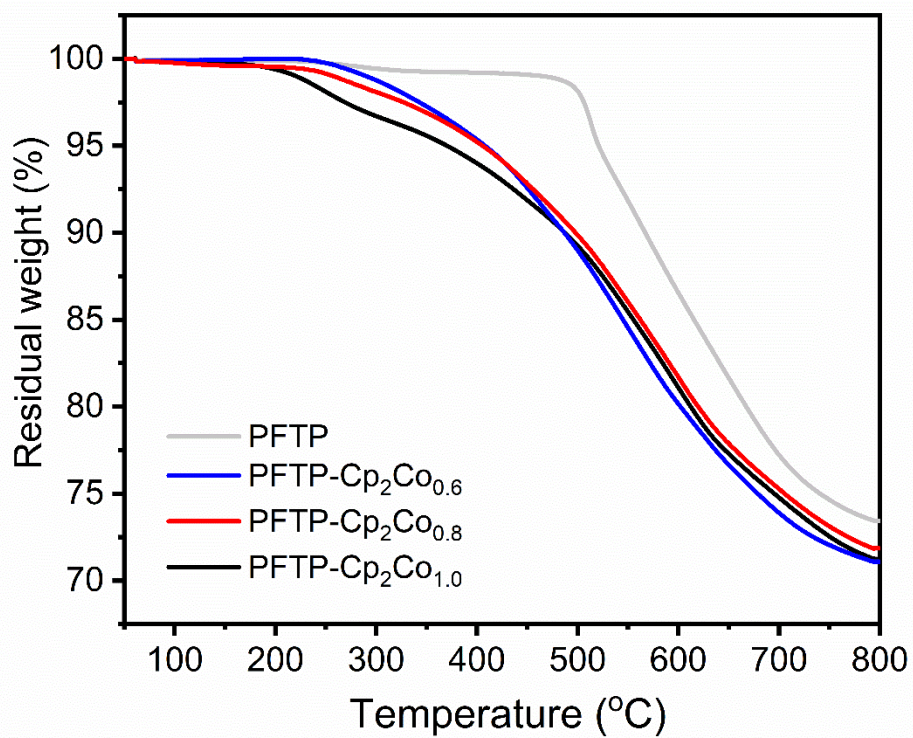
Fig. S14 TGA curves of PFTP membrane and PFTP-Cp_2Co_x membrane.
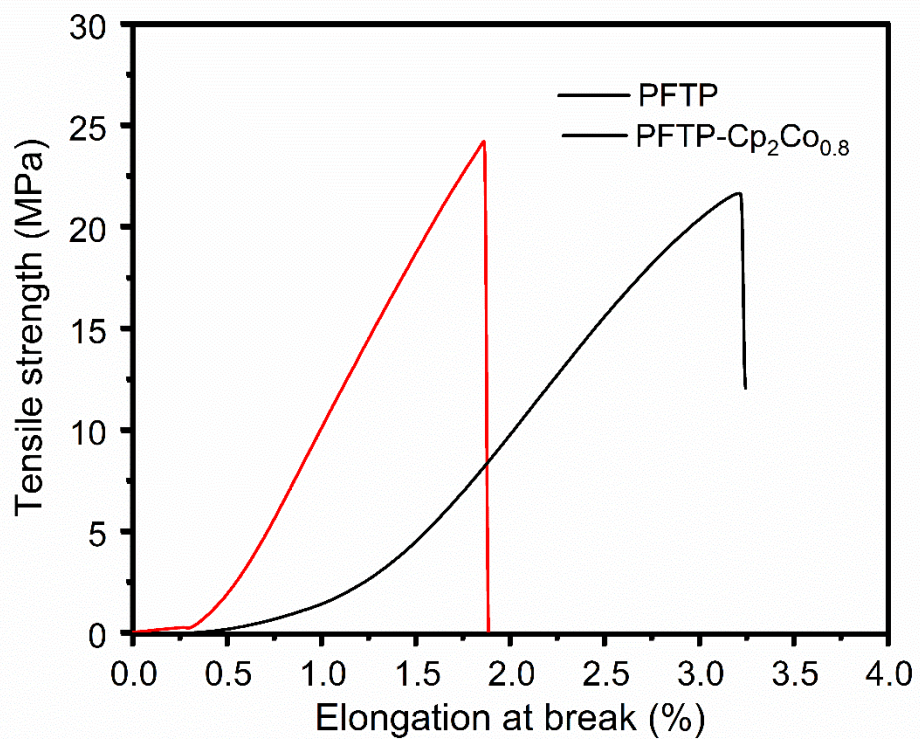
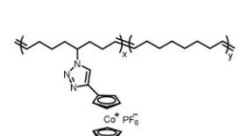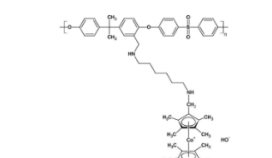**Fig. S15** Stress-strain curves of PFTP membrane and PFTP-Cp$_2$Co$_x$ membrane.
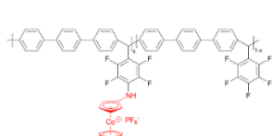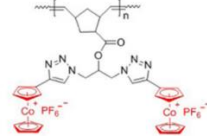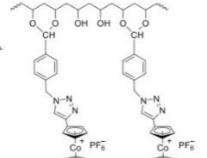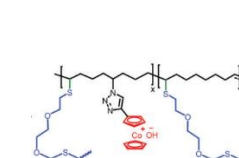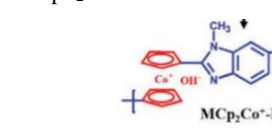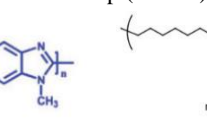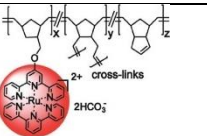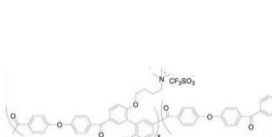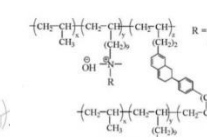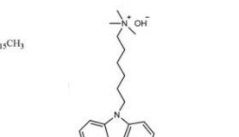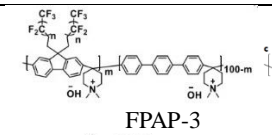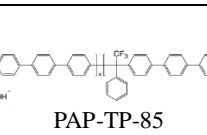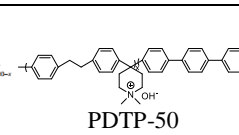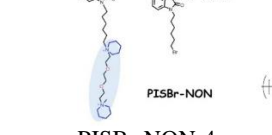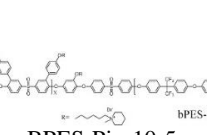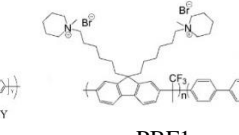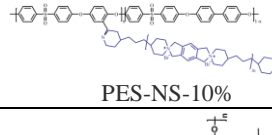
Table S1 Comparison of AEMFC performance of PFTP-Cp$_2$Co$_{0.8}$ and other metal-based and non-metal-based AEMs

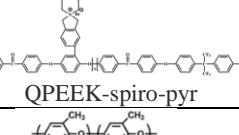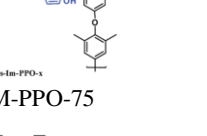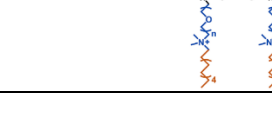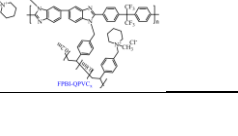| Cation	AEM	IEC[a] (mmol g^{-1})	σ (mS cm^{-1})	P$_{H_2/air}$ (mW cm^{-2})	P$_{H_2/O_2}$[b] (mW cm^{-2})	Ref
Cobaltocenium	PFTP-Cp$_2$Co$_{0.8}$	1.44	75.8 (80 ℃)	131	287	This work
	P2	1.73	41.8 (80 ℃)	-	90	5
	H-AEM$_{50}$-OH	1.86	90 (90 ℃)	-	-	6
	H-AEM$_{40}$-OH	1.53	72 (90 ℃)	-	-	
	Cp$^*_2$Co$^+$-PSf123	1.20	22 (RT)	-	-	7
	PVA-CoCp (1%GA)	1.21	17.7 (20 ℃)	-	179	8
	CL-AEM30-OH	1.07	53.3 (80 ℃)	-	-	9
	MCP$_2$Co$^+$-PBI	1.92	37.5 (90 ℃)	-	-	10
	omcAEM	-	83.7 (80 ℃)	-	350	11
Ruthenium	ttpRu-PN17	1.4	28.6 (30 ℃)	-	-	12
Quaternary ammonium (QA)	OBuTMA–AAEPs-1.0 (OH$^-$)	1.75	75 (60 ℃)	-	120 (50℃)	13
	PP-TMA-20	1.56	58.2 (80 ℃)	-	122	14
	QPC-TMA	2.06	125 (70 ℃)	-	1610	15
Piperidinium	FPAP-3	2.71	97 (40℃)	-	2000	16
	PAP-TP-85	2.35	163 (80 ℃)	-	920	17
	PDTP-50	2.54	158 (80 ℃)	1380	2580	18
	PISBr-NON-4	1.88	139.67 (80 ℃)	-	514.4	19
	BPES-Pip-10-5	2.04	105.8 (80 ℃)	-	136.9	20
	PBF1	1.94	69 (80 ℃)	-	410	21
N-spirocyclic QA	PES-NS-10%	1.75	95.5 (80 ℃)	-	110.1	22
	PPO-SDSU-36	1.91	51.6 (60℃)	-	90	23
	QPEEK-spiro-pyr	1.57	49.6 (80 ℃)	-	90	24
Imidazolium	Cross-IM-PPO-75	3.39	32 (80 ℃)	-	224.84	25
	IM-PEG-PPO-70	0.95	32.3 (80 ℃)	-	179	26
	2-ACPBI	1.75	91.2 (80 ℃)	-	631.5	27
	FPBI-QPVC2.5	2.42	91.7 (80 ℃)	-	197.5	28
Guanidinium	PPO-BG6-75	1.54	50 (80 ℃)	-	-	29
Quaternary phosphonium (QP)	TPQPOH	1.09	27 (20 ℃)	-	200	30

[a]Theoretical IEC.

[b]Test conditions: 80 ℃.

Table S2 Chemical structure of AEMs

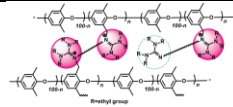| Cation	Chemical structure
Cobaltocenium	PFTP-C$_2$Co$_{0.8}$ (P2) H-AEM$_{50}$-OH Cp$^*_2$Co$^+$-PSf123 PVA-CoCp (1%GA) CL-AEM30-OH MCP$_2$Co$^+$-PBI omcAEM
Ruthenium	ttpRu-PN 17
Quaternary ammonium (QA)	OBuTMA–AAEPs-x (OH$^-$) PP-TMA-20 QPC-TMA
Piperidinium	FPAP-3 PAP-TP-85 PDTP-50 PISBr-NON-4 BPES-Pip-10-5 PBF1
N-spirocyclic QA	PES-NS-10% PPO-SDSU-36 QPEEK-spiro-pyr
Imidazolium	Cross-IM-PPO-75 IM-PEG-PPO-70

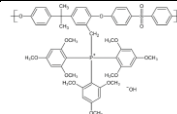|	2-ACPBI	FPBI-QPVC2.5	
Guanidinium		PPO-BG6-75	
Quaternary phosphonium (QP)		TPQPOH	

References

1   M. Jochriem, D. Bosch, H. Kopacka and B. Bildstein, *Organometallics*, 2019, **38**, 2278-2279.

2   X. Li, K. Yang, Z. Li, J. Guo, J. Zheng, S. Li, S. Zhang and T. A. Sherazi, *Int. J. Hydrogen Energy*, 2022, **47**, 15044-15055.

3   M. J. Frisch, G. W. Trucks, H. B. Schlegel, et al., *Gaussian 16 Revision*. A.03, Gaussian Inc., Wallingford, CT, 2016.

4   A. D. William Humphrey, and Klaus Schulten, *J. Mol. Graph.*, 1996, **14**, 33-38.

5   W. Yang, J. Yan, P. Xu, J. Chen, Q. Fang, D. Lin, Y. Yan and Q. Zhang, *Macromolecules*, 2022, **55**, 7763-7774.

6   T. Zhu, S. Xu, A. Rahman, E. Dogdibegovic, P. Yang, P. Pageni, M. P. Kabir, X. D. Zhou and C. Tang, *Angew. Chem. Int. Ed.*, 2018, **57**, 2388-2392.

7   S. Gu, J. Wang, R. B. Kaspar, Q. Fang, B. Zhang, E. Bryan Coughlin and Y. Yan, *Sci. Rep.*, 2015, **5**, 11668.

8   W. Yang, S. Liu, J. Yan, F. Zhong, N. Jia, Y. Yan and Q. Zhang, *Macromolecules*, 2021, **54**, 9145-9154.

9   T. Zhu and C. Tang, *Polym. Chem.*, 2020, **11**, 4542-4546.

10   N. Chen, H. Zhu, Y. Chu, R. Li, Y. Liu and F. Wang, *Polym. Chem.*, 2017, **8**, 1381-1392.

11   T. Zhu, Y. Sha, H. A. Firouzjaie, X. Peng, Y. Cha, D. Dissanayake, M. D. Smith, A. K. Vannucci, W. E. Mustain and C. Tang, *J. Am. Chem. Soc.*, 2020, **142**, 1083-1089.

12   Y. Zha, M. L. Disabb-Miller, Z. D. Johnson, M. A. Hickner and G. N. Tew, *J. Am. Chem. Soc.*, 2012, **134**, 4493-4496.

13   Z. Zhang, L. Wu, J. Varcoe, C. Li, A. L. Ong, S. Poynton and T. Xu, *J. Mater. Chem. A, 2013*, **1**, 2595-2601.

14   M. Zhang, J. Liu, Y. Wang, L. An, M. D. Guiver and N. Li, *J. Mater. Chem. A*, 2015, **3**, 12284-12296.

15   M. S. Cha, J. E. Park, S. Kim, S.-H. Han, S.-H. Shin, S. H. Yang, T.-H. Kim, D. M. Yu, S. So, Y. T. Hong, S. J. Yoon, S.-G. Oh, S. Y. Kang, O.-H. Kim, H. S. Park, B. Bae, Y.-E. Sung, Y.-H. Cho and J. Y. Lee, *Energy Environ. Sci.*, 2020, **13**, 3633-3645.

16   X. Wu, N. Chen, C. Hu, H. A. Klok, Y. M. Lee and X. Hu, *Adv. Mater.*, 2023, e2210432.

17   J. Wang, Y. Zhao, B. P. Setzler, S. Rojas-Carbonell, C. Ben Yehuda, A. Amel, M. Page, L. Wang, K. Hu, L. Shi, S. Gottesfeld, B. Xu and Y. Yan, *Nat. Energy*, 2019, **4**, 392-398.

18   N. Chen, C. Hu, H. H. Wang, S. P. Kim, H. M. Kim, W. H. Lee, J. Y. Bae, J. H. Park and Y. M. Lee, *Angew. Chem. Int. Ed.*, 2021, **60**, 7710-7718.

19   J. Zhang, W. Yu, X. Liang, K. Zhang, H. Wang, X. Ge, C. Wei, W. Song, Z. Ge, L. Wu and T. Xu, *ACS Appl. Energy Mater.*, 2021, **4**, 9701-9711.

20   B. Shen, B. Sana and H. Pu, *J. Membr. Sci.*, 2020, **615**, 118537.

21 R. Ren, S. Zhang, H. A. Miller, F. Vizza, J. R. Varcoe and Q. He, *ACS Appl. Energy Mater.*, 2019, **2**, 4576-4581.

22 F. H. Liu, Q. Yang, X. L. Gao, H. Y. Wu, Q. G. Zhang, A. M. Zhu and Q. L. Liu, *J. Membr. Sci.*, 2020, **595**, 117560.

23 J. Xue, X. Liu, J. Zhang, Y. Yin and M. D. Guiver, *J. Membr. Sci.*, 2020, **595**, 117507.

24 L. Shang, D. Yao, B. Pang and C. Zhao, *Inter. J. Hydrogen Energy*, 2021, **46**, 19116-19128.

25 B. Lin, F. Xu, F. Chu, Y. Ren, J. Ding and F. Yan, *J. Mater. Chem. A*, 2019, **7**, 13275-13283.

26 X. Zhang, J. Guo, X. Chu, C. Fang, Y. Huang, L. Liu and N. Li, *J. Membr. Sci.*, 2022, **659**, 120820.

27 X. Wang, J. Li, W. Chen, B. Pang, Y. Liu, Y. Guo, X. Wu, F. Cui and G. He, *ACS Appl. Mater. Interfaces*, 2021, **13**, 49840-49849.

28 C. Lin, J. Wang, G. Shen, J. Duan, D. Xie, F. Cheng, Y. Zhang and S. Zhang, *J. Membr. Sci.*, 2019, **590**, 117303.

29 B. Xue, Q. Wang, J. Zheng, S. Li and S. Zhang, *J. Membr. Sci.*, 2020, **601**, 117923.

30 S. Gu, R. Cai, T. Luo, Z. Chen, M. Sun, Y. Liu, G. He and Y. Yan, *Angew. Chem. Int. Ed.*, 2009, **48**, 6499-6502.